Nature of the superionic transition in Ag^+ and Cu^+ halides

D. A. Keen,[1,2] S. Hull,[2] A. C. Barnes,[3] P. Berastegui,[4] W. A. Crichton,[5] P. A. Madden,[6] M. G. Tucker,[7] and M. Wilson[8]
[1]*Physics Department, Oxford University, Clarendon Laboratory, Parks Road, Oxford OX1 3PU, United Kingdom*
[2]*ISIS Facility, Rutherford Appleton Laboratory, Chilton, Didcot, Oxon OX11 0QX, United Kingdom*
[3]*H H Wills Physics Laboratory, Tyndall Avenue, Bristol, BS8 1TL, United Kingdom*
[4]*Arrhenius Laboratory, Stockholm University, S-106 91 Stockholm, Sweden*
[5]*ESRF, BP220, F-38043 Grenoble Cedex, France*
[6]*Physical and Theoretical Chemistry Laboratory, Oxford University, South Parks Road, Oxford, OX1 3QZ, United Kingdom*
[7]*Department of Earth Sciences, Cambridge University, Downing Street, Cambridge CB2 3EQ, United Kingdom*
[8]*University College London, Department of Chemistry, Christopher Ingold Laboratories, 20 Gordon Street, London, WC1H 0AJ, United Kingdom*

(Received 31 January 2003; revised manuscript received 23 May 2003; published 30 July 2003)

Silver and copper halides generally display an abrupt (first-order) transition to the superionic state. However, powder diffraction studies and molecular dynamics (MD) simulations of AgI under hydrostatic pressure both indicate that a continuous superionic transition occurs on heating. The gradual onset of the highly conducting state is accompanied by an increasing fraction of dynamic Frenkel defects, a peak in the specific heat and anomalous behavior of the lattice expansion. Similar methods have been employed to investigate the proposed continuous superionic transition between the two ambient pressure face centered cubic phases of CuI. This is difficult to examine experimentally, because the hexagonal β phase exists over a narrow temperature range between the γ (cation ordered) and α (cation disordered) phases. MD simulations performed with the simulation box constrained to remain cubic at all temperatures show that, although limited Cu^+ Frenkel disorder occurs within γ-CuI, CuI undergoes an abrupt superionic transition at 670 K to the superionic α phase. This is supported by powder neutron diffraction studies of CuI lightly doped with Cs^+ to prevent stabilization of the β phase. The implications of these results on the phase transitions of other copper and silver halide superionic conductors are discussed.

DOI: 10.1103/PhysRevB.68.014117 PACS number(s): 61.43.−j, 64.70.−p, 61.10.−i, 61.12.−q

I. INTRODUCTION

Superionic conductors are compounds which exhibit exceptionally high values of ionic conductivity σ (typically $\sigma \sim 0.1-1\ \Omega^{-1}\,\mathrm{cm}^{-1}$) in the solid state.[1] The two most widely studied families of superionic conductor are the fluorite structured compounds and the Ag^+/Cu^+ halides. The former includes numerous fluorides, chlorides and oxides and is typified by β-PbF_2. The ideal cubic fluorite structure (space group $Fm\bar{3}m$) possesses a face centered cubic (fcc) sublattice of cations (Pb^{2+}), in which all the tetrahedral interstices are filled with anions (F^-) and the octahedral holes are empty (see Fig. 1). If β-PbF_2 is heated above $\sim$600 K it undergoes a type-II superionic transition (in the notation of Boyce and Huberman[2]) in which an increasing fraction of anions become delocalized from the lattice sites and form dynamic Frenkel defects.[3–5] The onset of this anion disorder gives rise to a rapid increase in the F^- diffusion coefficient with temperature,[5,6] associated anomalies in the lattice expansion dV/dT[4,5,7,8] and a so-called λ-type peak in the specific heat C_p (Ref. 5,9,10) [whose maximum defines the superionic transition temperature, $T_c = 711$ K in β-PbF_2 (Ref. 9)]. On further heating above T_c the percentage of anions leaving the regular lattice sites increases, before saturating at a value of $\sim$25%.[4] The latter behavior is generally interpreted as evidence for repulsive interactions between defects[11] and causes σ to level off at $\sim 3\ \Omega^{-1}\,\mathrm{cm}^{-1}$.

The behavior of the Ag^+ and Cu^+ halide superionics is in marked contrast to the above description. In the archetypal case of AgI, the material generally exists under ambient conditions as a two phase mixture of the β and γ phases.[12] These adopt the hexagonal wurtzite ($P6_3mc$) and cubic zincblende ($F\bar{4}3m$) structures, respectively, and can be described as hexagonal close packed (hcp) and fcc anion sublattices in which the cations are ordered over half the tetrahedral holes such that the tetrahedra containing a cation only share corners (for the case of γ-AgI, either the $T1$ or $T2$ sites are filled in Fig. 1). Heating AgI causes a first-order structural phase transition to the superionic α phase at 420 K, in which σ increases by around three orders of magnitude and the anion sublattice forms a body centered cubic (bcc) array (for a review, see Ref. 13). This is a typical example of a type-I superionic transition.[2] In α-AgI the two Ag^+ per unit cell predominantly occupy the 12 tetrahedral sites per unit cell and undergo rapid jump diffusion between them.[14–16] This occurs in $\langle 110 \rangle$ directions via the trigonal interstices rather than in $\langle 100 \rangle$ directions via the octahedral ones.[16] On increasing temperature there is little change in the structure and σ is essentially constant at $\sim 2\ \Omega^{-1}\,\mathrm{cm}^{-1}$ up to the melting point of 825 K, above which σ falls by $\simeq 10\%$.[17]

First-order (type-I) superionic transitions are a common feature within the tetrahedrally coordinated members of the Ag^+ and Cu^+ halides. CuCl, CuBr, and CuI all adopt the

cubic zinc blende (γ-AgI) structure and undergo first-order structural phase transitions to a superionic state on heating and, in some cases, first-order structural transitions between superionic phases (for details, see Ref. 18). The superionic phases are all characterized by dynamic cation disorder between the tetrahedral interstices formed by bcc [α-CuBr,[19] CuCl-III,[20] and CuI-VII (Ref. 21)], hcp [β-CuBr (Ref. 19)], and fcc (α-CuI,[22] with both $T1$ and $T2$ sites half-filled in Fig. 1) anion sublattices. By contrast, AgF, AgCl, and AgBr adopt the octahedrally coordinated rocksalt structure ($Fm\bar{3}m$) characteristic of ionic compounds (Fig. 1, Ag^+ in O sites) and do not possess high temperature superionic phases (but see Sec. II A). A general discussion of disorder within superionic conductors, including the importance of other experimental (e.g., XAS) and computer modeling (e.g., RMC) methods not considered here is contained in a recent review.[23]

While simplistic, the descriptions given above highlight the significant differences in the superionic behavior between the fluorite structured compounds and the Ag^+/Cu^+ halides. It is important to assess to what extent these represent differences in the fundamental processes which underlie the development of the thermally induced disorder within each family of compounds. Such considerations are particularly timely, in view of recent attempts to provide semiempirical models of the superionic transition mechanism based on an additional term in the chemical potential proportional to the cube root of the defect concentration[24,25] or structural considerations involving coupling between mobile and immobile sublattices.[26]

The rest of the paper is organized by considering octahedrally coordinated AgI and tetrahedrally coordinated CuI in turn. First, the background to the superionic behavior of the high-pressure rocksalt structured phase of AgI (AgI-III) is described, together with results from recent x-ray diffraction and molecular dynamics (MD) simulations. These are discussed with reference to the established behavior of β-PbF_2 and show that genuine type-II superionic behavior is observed in AgI-III. Secondly, a similar investigation of CuI is described, again including temperature-dependent MD simulations and, in addition, recent results from neutron diffraction measurements of Cs-doped CuI. These are used to show that the hypothetical $\gamma \leftrightarrow \alpha$ superionic phase transition is actually of first-order (type-I). These two sections are then followed by a more general discussion, outlining the differences between AgI-III and CuI and some necessary structural conditions for type-II and type-I behavior.

A Sites	Type	Structure
O	*AX*	rocksalt
T1 or T2	*AX*	zincblende
T1 and T2	*AX*	α-CuI
T1 and T2	XA_2	fluorite

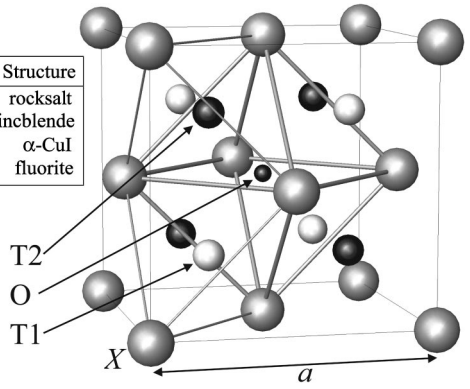

FIG. 1. Schematic diagram of an fcc sublattice of X ions, showing the octahedral cavities (O) and two sets of tetrahedral cavities ($T1$ and $T2$). The crystal structures formed by filling these cavities with A counterions in various ways are given. In the case of α-CuI, the tetrahedral sites $T1$ and $T2$ are 50% occupied on average. The length of the lattice parameter a is also shown.

II. ROCKSALT STRUCTURED SILVER IODIDE

A. Background

Although rocksalt structured AgBr does not undergo a type-I transition to a superionic phase at elevated temperatures, its ionic conductivity increases rapidly in the temperature region $\sim$100–150 K below T_m ($=701$ K), reaching a value $\sigma \sim 0.5\ \Omega^{-1}\,\mathrm{cm}^{-1}$.[17] Neutron diffraction studies at temperatures up to 0.3 K below T_m indicated that the Ag^+ vibrate anisotropically about the O positions but with an increasing occupancy of the $T1$ and $T2$ positions as T_m is approached.[27] Just below T_m the concentration of cation Frenkel defects is $\sim 4\%$.[27] It has been proposed[28] that AgBr starts to undergo a type-II superionic transition which is interrupted by the melting transition before the highly disordered state (of the type observed in β-PbF_2) is reached. The premature melting of AgBr may be due to the coincident formation of a small (but significant) concentration of Schottky defects, which induces disorder on the anion sublattice and promotes melting.[28]

A more informative example of a possible type-II superionic transition within the Ag^+/Cu^+ halides is provided by the application of hydrostatic pressure to AgI. The p-T phase diagram in AgI has recently been reexamined using x-ray diffraction.[29] At $p=0.28$ GPa, AgI transforms to the rocksalt structured phase AgI-III.[30] AgI-III is isostructural with AgBr and the $\beta+\gamma \rightarrow$ III transformation changes the coordination of both anions and cations from 4 to 6. Despite the significant increase in the density [by almost 20% (Ref. 30)], measurements of the ionic conductivity of AgI under pressure[31] indicated a rapid, though gradual, increase in σ within the rocksalt structured phase with increasing temperature, prior to transformation to the bcc structured superionic α phase. Molecular dynamics (MD) simulations provided conflicting evidence for[32,33] and against[34] the onset of Ag^+ disorder within AgI-III. However, confirmation of a type-II transition within rocksalt structured AgI-III was recently provided by neutron powder diffraction studies at $p=1.1$ GPa,[35] showing an increasing fraction of Ag^+ leaving the octahedral O sites and residing in the tetrahedral ($T1$ and $T2$) voids at temperatures above $T \simeq 500$ K. The extent of Ag^+ disorder reaches $\sim$30% in AgI-III at 700 K and there was evidence of an anomalous increase in the lattice parameter of the type observed in β-PbF_2.

B. X-ray diffraction from AgI-III

X-ray powder diffraction studies of AgI-III were performed on the beamline ID30 (Ref. 36) at the ESRF, Grenoble using a 100 μm beam of wavelength λ

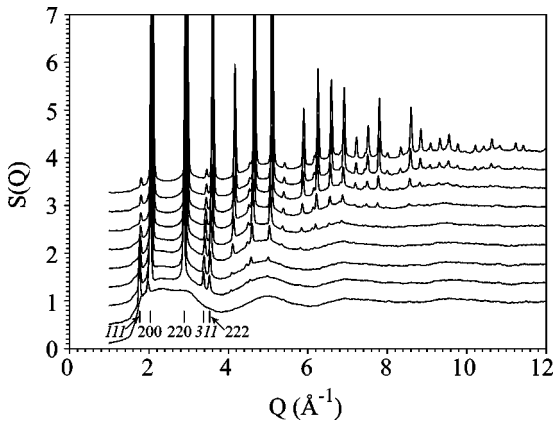

FIG. 2. X-ray total scattering structure factors $S(Q)$, from AgI at $p=2.6(2)$ GPa and 983 K (molten) and 963, 873, 773, 673, 573, 473, 373, and 293 K (phase-III). The approximate positions of some Bragg reflections are marked and data from each successive temperature have been offset by $+0.4$ for clarity.

$=0.15815$ Å. A cylindrical sample of 0.9 mm diameter and 2.0 mm height was placed inside a BN container which in turn was inside a cylindrical graphite heater surrounded by a boron epoxy gasket. The complete assembly was loaded inside a Paris-Edinburgh large-volume pressure cell.[37] Data were collected at a pressure of $p=2.6(2)$ GPa and at temperatures up to 963(3) K on a sample which had already been heated and cooled at pressure, using a two-dimensional image plate system covering the scattering angles $0°\leqslant 2\theta \leqslant 27°$. An oscillating set of soller slits was used between the sample and the image plate to reduce the background signal from the pressure cell components. Pressures were determined from an identical measurement of the BN sample container and the known pressure and temperature behavior of the BN lattice parameters.[38] The temperature was measured using a type-K thermocouple, to which no pressure correction was made, placed in the wall of the BN sample container. Data from the 2D image plate were corrected for spatial distortion and were summed to produce a 1D powder pattern using the program FIT2D.[39] A proportion of the BN measurement was subtracted from the data to account for the background transmitted through the soller collimator and the background subtracted data were normalized in the usual way to produce total scattering structure factors.[40]

A selection of total scattering structure factors from the experimental data collected on increasing temperature is shown in Fig. 2. The diffuse scattering increases and the high-Q Bragg peak intensities decrease significantly as the temperature is raised, clearly indicating an increase in thermally induced disorder. There is also a change in the relative intensities of the Bragg reflections over the measured temperature range, whereby those with $h+k+l=2n$ decrease and those with $h+k+l=2n+1$ increase as temperature increases. The intensities of $h+k+l=2n+1$ rocksalt peaks are primarily determined by the difference between the mean scattering powers of the cation and anion sites. Since both are filled at ambient temperature and the x-ray form factors for Ag^+ and I^- are very similar, the structure factor for these peaks is very low. However, as the mean occupancy of the

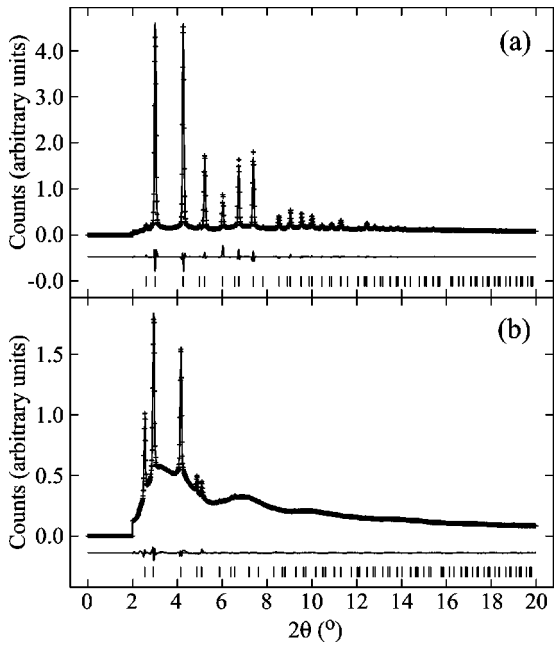

FIG. 3. Least squares refinements of the x-ray diffraction data collected from AgI at 2.6 GPa and (a) $T=293$ K and (b) 963 K. The points are the experimental data and the solid line through the points is the best fit as described in the text. The lower trace shows the difference and the tick marks across the bottom indicate the positions of the expected reflections based on the rocksalt structure.

Ag^+ sites falls when the material enters its superionic state, this cancellation no longer applies and the intensity of reflections such as 111 and 311 increases (see Fig. 2).

Rietveld refinements of the data were carried out using the rocksalt structure and allowing the relative proportion of cations on O and $(T1+T2)$ sites to vary. Initial refinements at room temperature showed $\sim 12\%$ occupation of tetrahedral sites. This is inconsistent with the earlier neutron diffraction results[35] and is the result of preferred orientation within the sample, which could be seen in the slight ''speckling'' in diffraction rings in the 2D data images. In order to test this, an additional run at a similar pressure was carried out on a sample which had not been heated. The 2D data image from this control sample showed smooth, untextured diffraction rings, no evidence for partial recrystallization and a good fit to the diffraction pattern was obtained with a model with no cations occupying tetrahedral sites. In order to account for the preferred orientation, the room temperature data from the ''textured'' sample were refined with an ideal rocksalt structure (i.e., the tetrahedral sites were unoccupied) and a spherical harmonic preferred orientation correction. This provided a very good fit to the data (see Fig. 3). Inspection of the higher temperature data sets suggested that the degree of preferred orientation did not change significantly and hence all data sets were refined using a preferred orientation correction which was fixed to the values determined from the room-temperature data.

Figures 4(a) and 4(a) inset show the temperature dependence of the volume per formula unit (V/Z) and linear expansivity, respectively. There is clear evidence of anomalous behavior in V/Z at $T\sim 800$ K corresponding to a peak in

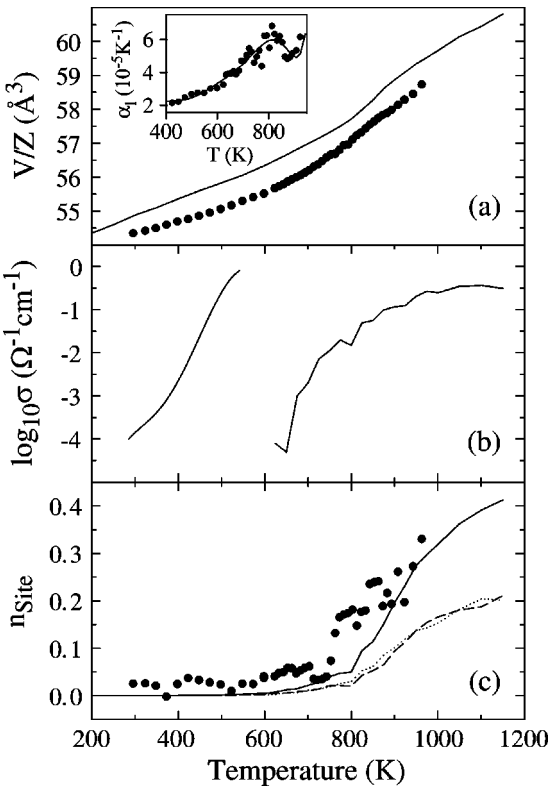

FIG. 4. Summary of the temperature dependent MD simulations of rocksalt structured AgI-III and comparable experimental data. (a) The simulated volume per formula unit (V/Z) obtained by MD simulations at $p=2.5$ GPa (line) and x-ray diffraction at $p=2.6$ GPa (points). The inset shows the linear expansivity from the x-ray data. The line corresponds to the derivative of a polynomial fit to the lattice parameter and the points were obtained from the slope defined by the lattice parameters measured at next lowest and next highest temperatures. (b) The simulated ionic conductivity at $p=2.5$ GPa (right-hand curve) and the measured data at $p=0.9$ GPa (Ref. 31) (left-hand curve). (c) The occupancies of the $T1$ (dashed line), $T2$ (dotted line), and $T=T1+T2$ (full line) sites obtained by polyhedral analysis of the simulated Ag^+ motions at $p=2.5$ GPa, compared with the T site occupancy from experimental x-ray diffraction results at $p=2.6$ GPa (points).

dV/dT. Figure 4(c) also shows the interstitial occupancy as a function of temperature. At low temperatures it is approximately constant at $\sim 2.5\%$, and above ~ 700 K it increases significantly. These results are wholly consistent with the earlier neutron diffraction results and the established phase diagram of AgI. The higher pressure of the x-ray results leads to a higher temperature for the onset of disorder, a wider temperature range within the disordered regime, followed by melting rather than transformation to the α phase.

It should be possible to use the total scattering data to investigate the local environment around the Ag^+ interstitials, similar to the earlier work on AgBr.[27] However, without extremely high quality data to high Q, it is very difficult to carry out reliable reverse Monte Carlo (RMC) refinements, particularly since the rocksalt structure has many common near neighbor distances and the resulting RMC model would not be well constrained.[41] Despite this, approximate total radial distribution functions do show a shortening of the lowest-r peak with increasing temperature, shifting from $r \simeq 2.95$ Å$\simeq a/2$ at room temperature to $r \simeq 2.75$ Å$\simeq \sqrt{3}a/4$ just below melting. The former of these corresponds to octahedral Ag-I distances and the latter to tetrahedral Ag-I distances or the distance between Ag^+ ($T1$ or $T2$) and Ag^+ in O sites. This shows an increasing tendency for tetrahedral coordination over octahedral coordination as temperature increases, but it is not sufficient to assess the local Ag^+-Ag^+ correlations in a manner that has been done for CuI (see Sec. IV)

C. MD simulation of AgI-III

Complementary MD simulations of the behavior of rocksalt structured AgI on increasing temperature have been performed at 31 temperatures in the range $50 \leqslant T(\mathrm{K}) \leqslant 1150$, with particular emphasis on the region $600 \leqslant T(\mathrm{K}) \leqslant 1000$ where the superionic transition occurs. All simulations were performed at a pressure of $p=2.5$ GPa and melting was observed to occur at $T=1200$ K. The well established RVP potentials[14,42] have (in slightly different forms) proved particularly successful in reproducing the structure and dynamics of superionic α-AgI,[14] including the nature of the $\beta \leftrightarrow \alpha$ transition,[42–45] possible order-disorder phenomena within α-AgI (Ref. 46) and the various boundaries in the p-T phase diagram.[32–34] Its original form[14] is adopted here. The simulation box comprised $4\times4\times4$ unit cells, containing a total of 512 ions and periodic boundary conditions were applied. The simulations were allowed to equilibrate for $\simeq 60$ ps and then a subsequent run of $\simeq 60$ ps was used for analysis of the ionic motions. The mean distribution of ions within the unit cell was determined by averaging over time t and over all the unit cells in the simulation box. The cation diffusion coefficient D_{Ag}, was obtained from the slope of the mean squared displacement at long times, i.e.,

$$D_{\mathrm{Ag}} = \lim_{t\to\infty} \frac{1}{6N_{\mathrm{Ag}}t} \left\langle \sum_{j=1}^{N_{\mathrm{Ag}}} [r_j(t) - r_j(0)]^2 \right\rangle,$$

where N_{Ag} is the number of Ag^+ and $r_j(t)$ is the position of cation j at time t. Assuming that only the cations contribute to the ionic conductivity, σ can then be estimated using the expression $\sigma = c_{\mathrm{Ag}} D_{\mathrm{Ag}} q_{\mathrm{Ag}}^2 / kT$, where c_{Ag} is the concentration of Ag^+ which have ionic charge q_{Ag}. This approach neglects correlations between mobile ions and, since the Haven's ratio of many superionics is not unity,[5,47] correlated motions are to be expected. However, it is the trend with temperature that is most important here, and this is effectively reproduced by the model.

The values of the volume per formula unit (V/Z) obtained during the MD simulations are illustrated in Fig. 4(a). The anomalous behavior of the lattice expansion is clearly observed, though at a somewhat higher temperature than observed experimentally. In addition, the higher temperature attained during the simulations prior to melting indicates a reduction in the expansion coefficient at $T \geqslant 1000$ K, providing a better agreement with the situation observed in β-PbF_2, where there is a peak in dV/dT at ~ 700 K which is

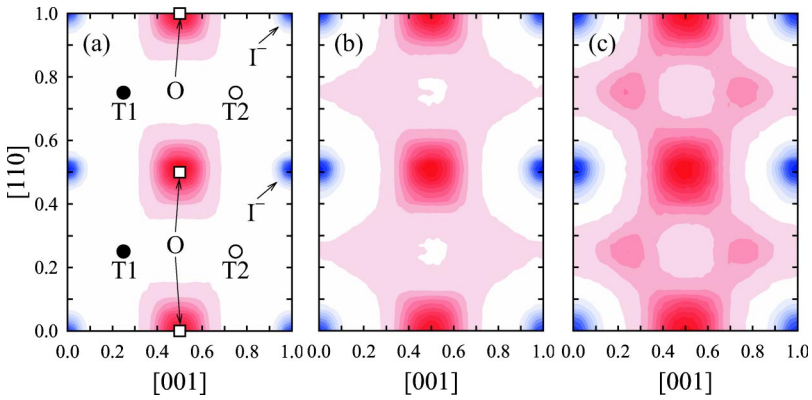

FIG. 5. (Color online) The simulated density of I^- and Ag^+ within the $(1\bar{1}0)$-plane of AgI-III at temperatures of (a) 700, (b) 900, and (c) 1100 K. The I^- density is centered at 000 and $\frac{1}{2}\frac{1}{2}0$, etc. All other contours correspond to Ag^+ density. The densities are calculated within a slice of thickness 0.1 perpendicular to the plane. The locations of the octahedral (O) and tetrahedral ($T1$ and $T2$) sites are illustrated in plot (a).

almost coincident with the superionic transition temperature, defined by the peak in C_p.[9] Calculations of the cation diffusion coefficient D_{Ag} indicate the onset of cation disorder at $T \sim 650$ K, with clear evidence of diffusion of Ag^+. The estimated values of σ are compared with the published data[31] in Fig. 4(b) and, when allowance is made for the differing pressures and the approximations inherent in this approach, the agreement between the measured and calculated values is impressive.

Sections through the $(1\bar{1}0)$ plane of the simulated ionic density at temperatures of 700, 900, and 1100 K are illustrated in Fig. 5. A gradual redistribution of Ag^+ density from the O sites to the $T1$ and $T2$ sites occurs on increasing temperature. This indicates that cation diffusion occurs between the O positions via the T sites (i.e., hops in $\langle 111 \rangle$ directions), and is confirmed by direct studies of the motions of individual ions within the simulations. To quantify the extent of the thermally induced disorder within AgI-III on increasing temperature it is necessary to estimate the occupancies of the O, $T1$, and $T2$ positions. For this purpose a polyhedral analysis method of the type used previously[48,49] is adopted. At each time step the simulation box is divided into octahedra and (two types of) tetrahedra formed by the instantaneous positions of the anions surrounding the O, $T1$, and $T2$ sites. This process completely fills all the available space. Each cation is then assigned to lie inside one of these polyhedra and, after averaging over all timesteps and all cations, the average occupancies of the O, $T1$, and $T2$ centered polyhedra are obtained. As noted previously,[50] care must be taken when using this approach, since the simulated fraction of cations within (say) the anion octahedra cannot be directly compared with the occupancy of the sites at the center of these octahedra measured by diffraction techniques. Nevertheless, this method provides a straightforward approach to visualise the ionic conduction process. Previous discussions comparing the defect concentrations in PbF_2 obtained from MD and diffraction studies are also noted. Again apparent discrepancies occur when the definition of the defect concentration is inconsistent.[5,6]

The temperature variation of the simulated cation occupancies of the $T1$ and $T2$ sites is illustrated in Fig. 4(c), together with the total occupancy of the T sites (i.e., $T1 + T2$). The population of Ag^+ on the $T1$ and $T2$ sites is the same (within the uncertainties inherent in the low statistics) consistent with the space group being $Fm\bar{3}m$ rather than $F\bar{4}3m$, in accord with experimental data. The temperature dependence of the Frenkel Ag^+ disorder is comparable with that observed experimentally [see Fig. 4(c)], although the onset of T site occupation occurs at a slightly higher temperature in the MD simulations and experimentally AgI-III melts before the Ag^+ disorder reaches the higher values obtained in the MD studies.

The internal energy of the simulations is used to calculate the specific heat of the system C_p since this is a difficult quantity to determine experimentally under high pressure conditions. As illustrated in Fig. 6, there is a broad peak centered at $T \sim 800$ K. It is clear that the picture of the evolution of thermally induced cation disorder in rocksalt structured AgI-III provided by the MD simulations (and verified with reference to the available experimental data) is of a type-II superionic transition which bears a remarkable similarity to that observed in the anion conducting fluorite structured compounds. In particular, the presence of a peak in C_p, a maximum in the volume expansion dV/dT and the onset of

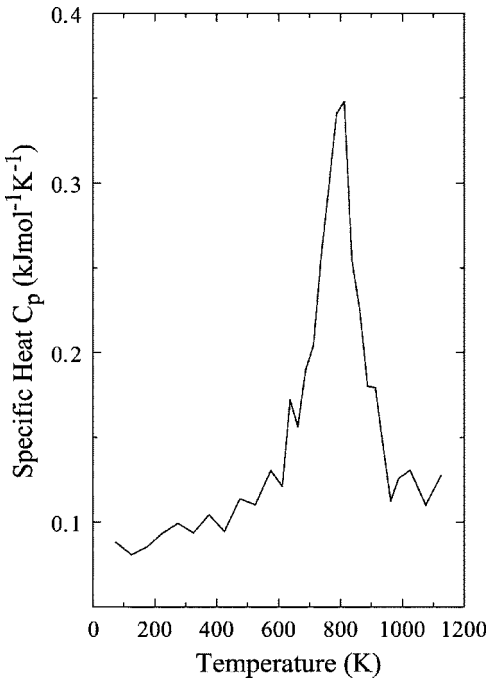

FIG. 6. The calculated temperature dependence of the specific heat C_p of rocksalt structured AgI-III at $p = 2.5$ GPa, determined from the internal energy of the MD simulations.

significant levels (few %) of dynamic Frenkel defects at comparable temperatures (i.e., the superionic transition temperature T_c) are common to both AgI-III ($T_c \sim 800$ K simulated at $p = 2.5$ GPa) and β-PbF_2 [observed at $T_c = 711$ K (Ref. 9)], as is the saturation of the defect concentration above T_c and the corresponding tendency of the temperature dependence of the ionic conductivity to level off.

III. FACE CENTERED CUBIC COPPER IODIDE

A. Background

Heating CuI at ambient pressure causes the low temperature zinc blende structured γ phase to transform to the β and α phases at temperatures of 643 and 673 K, respectively, prior to melting at 878 K.[51] The structure of the β phase has an hcp anion sublattice with the Cu^+ distributed in approximately the ratio 85:15 over two sets of tetrahedral interstices within space group $P\bar{3}m1$.[52] The high-temperature α-CuI phase is superionic, with an fcc anion sublattice and the Cu^+ randomly distributed over all the tetrahedral holes ($T1$ and $T2$ in Fig. 1) with 50% mean site occupancy and no significant occupancy of the octahedral (O) positions.[51] MD simulations indicate that the Cu^+ undergo extensive anharmonic thermal vibrations in the $\langle 111 \rangle$ directions (i.e., towards the O sites) but that diffusion occurs in $\langle 100 \rangle$ directions between nearest-neighbor T positions.[50,53–55]

X-ray diffraction studies of CuI on increasing temperature showed that extrapolation of the temperature dependence of the intensities of the Bragg peaks observed in the γ phase across the ''gap'' in which the β phase is observed met those measured in the α phase.[56] This suggests that the $\gamma \rightarrow \alpha$ transition could be a type-II superionic transition, interrupted by the presence of the two first-order $\gamma \rightarrow \beta$ and $\beta \rightarrow \alpha$ transitions. Support for this notion was provided by evidence of the onset of Cu^+ disorder within γ-CuI at temperatures below the $\gamma \rightarrow \beta$ transition by ionic conductivity,[57] NMR,[58] Raman,[59] MD,[50,53–55] and neutron diffraction[51] methods. The latter two techniques indicated that $\sim 5\%$ of Cu^+ leave the zinc blende lattice sites ($T1$) at temperatures immediately below the $\gamma \rightarrow \beta$ transition and reside on the alternative ($T2$) set of tetrahedral cavities. Conversely, calorimetry measurements[56] and the earliest MD simulations of CuI (Ref. 60) both showed that γ-CuI and α-CuI have substantially different lattice energies, consistent with a type-I transition. It has been suggested[61] that the β phase might be eliminated under pressure. However, subsequent diffraction measurements indicated that at $p \geqslant 0.3$ GPa the $\gamma \rightarrow \alpha$ transition does not become second-order but, instead, occurs via a different intermediate phase with rhombohedral symmetry.[21]

B. MD simulations of CuI

To investigate the nature of the superionic transition further, MD simulations of CuI have been performed at $p = 0$ GPa and over the temperature range $50 \leqslant T(\mathrm{K}) \leqslant 950$, the latter being slightly below the (simulated) melting temperature. The simulation box was constrained to be cubic, thus suppressing any tendency for the anion sublattice to transform from fcc to hcp. To probe the nature of the $\gamma \rightarrow \alpha$ transition, simulations were performed in temperature steps of 10 K in the temperature range $600 \leqslant T(\mathrm{K}) \leqslant 700$. In other respects, the MD simulations of CuI were the same as those described for AgI-III in Sec. II C.

The choice of interionic potentials for CuI is rather less straightforward than for AgI. While the same basic formalism is used, conflicting parameterisations of the various terms have been reported.[48,50,53–55,60,62] In particular, the simulated structural and ionic diffusion behavior appears rather sensitive to the value of the fractional ionic charge used.[62] Furthermore, it is difficult to derive a satisfactory set of potentials to describe the behavior of β-CuI as well as that of the two cubic γ and α forms.[53] It has also recently been reported that MD simulations of α-CuI fail to recreate some details of the radial distribution functions $g_{\mathrm{CuCu}}(\mathrm{r})$ and $g_{\mathrm{CuI}}(\mathrm{r})$ determined by neutron diffraction and EXAFS methods[63] (though there are also some differences between the results provided by these two experimental approaches). In this work the form originally proposed for CuI is adopted,[60] since the emphasis is on the nature of the superionic transition rather than the β phase or details of short-range correlations between diffusing ions.

The results of the MD simulations of CuI at temperatures close to the $\gamma \rightarrow \alpha$ transition are summarized in Fig. 7 and the ionic density within the $(1\bar{1}0)$ plane at temperatures of 500, 660, and 670 K is illustrated in Fig. 8. At low temperatures the Cu^+ reside exclusively on the $T1$ sites [Fig. 8(a)]. Starting at $T \simeq 620$ K, there is a slight increase in the lattice expansion [Fig. 7(a)] and the onset of limited Cu^+ disorder. The latter is characterized by an increasing fraction of cations occupying the alternative $T2$ set of tetrahedral interstices [Figs. 7(c) and 8(b)] and results in an increase in the ionic conductivity [Fig. 7(b)]. The small, but significant occupancy of the O positions in Fig. 7(c) (note break in scale) is an artifact of the polyhedral method of analysis, since the Cu^+ diffuse predominantly between nearest-neighbor T sites in $\langle 100 \rangle$ directions via the peripheries of the octahedral voids but the central octahedral site is a density minimum.[54] The simulations thus far appear to suggest that γ-CuI starts to undergo a type-II superionic transition on increasing temperature, in agreement with the experimental studies discussed above.[50,51,53–55,57–59] The extent of Cu^+ Frenkel disorder is predicted to reach $\sim 10\%$ at $T = 660$ K [Fig. 7(c)].

At $T = 670$ K an abrupt transition to a highly disordered structure occurs within ~ 10 ps of the start of the simulation. As illustrated in Fig. 8(c), the resultant configuration comprises a random distribution of the Cu^+ over both the $T1$ and $T2$ sites and represents the experimentally observed α phase of CuI. The $\gamma \rightarrow \alpha$ transition results in an abrupt increase in the volume per formula unit [Fig. 7(a)] and ionic conductivity [Fig. 7(b)].

The rather surprising presence of a type-I superionic $\gamma \rightarrow \alpha$ transition at $T = 670$ K within the simulations of CuI cannot, of course, be directly compared with the experimental data as the transformation is ''hidden'' by the β phase. Comparison of the behavior of the experimental volumes per formula unit at temperatures below and above the β phase

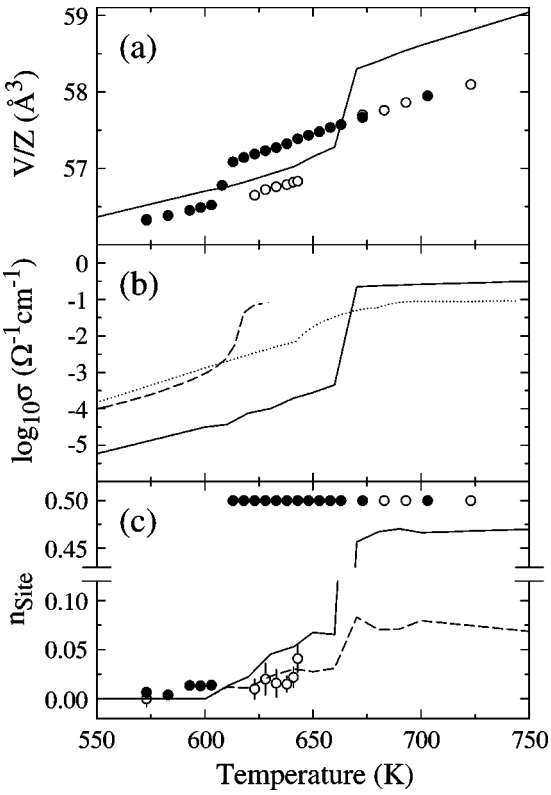

FIG. 7. Summary of the temperature dependent MD simulations of CuI at $p=0$ GPa and comparable ambient pressure experimental data. (a) The simulated volume per formula unit (V/Z) obtained by MD simulations (line) and neutron diffraction studies of pure CuI (open circles) (Ref. 51) and $Cu_{1-x}Cs_xI$ (filled circles). (b) The simulated ionic conductivity (full line) and measured data for pure CuI (Ref. 64) (dotted line) and $Cu_{1-x}Cs_xI$ (dashed line). (c) The occupancies of the $T2$ (full line) and O (dashed line) sites obtained by polyhedral analysis of the simulated Cu^+ motions in CuI, compared with the occupancies of the $T2$ sites from experimental neutron diffraction for pure CuI (open circles) (Ref. 51) and $Cu_{1-x}Cs_xI$ (filled circles).

stability region[51] tend to support the simulated behavior [Fig. 7(a)], though the MD simulations predict values within the α phase which are slightly too large. Also, the experimental ionic conductivity of CuI (Ref. 64) shows an increase within the γ phase and is relatively constant within the α phase, though quantitatively the agreement with the MD simulation results is rather poor.

C. Neutron diffraction of $Cu_{1-x}Cs_xI$

Experimental support for the presence of a type-I transition is, however, provided by chemical doping studies of CuI. In the course of extensive studies of the ternary phases formed by adding K^+, Rb^+ and Cs^+ to the Ag^+ and Cu^+ halides, it was observed that the addition of Cs^+ to CuI eliminates the β phase. It is not clear whether the modification to the sequence of thermally induced phase transitions in CuI is a volume (negative pressure) effect or a consequence of Cs^+ inhibiting the shearing of the close packed planes which presumably occurs at the fcc$\rightarrow$hcp ($\gamma\rightarrow\beta$) transition. As expected, in light of the significant size difference between Cs^+ and Cu^+, the solid solution region is very small. It is, therefore, reasonable to treat the Cs^+ dopant as a passive structural modifier, and consider the structural behavior of $Cu_{1-x}Cs_xI$ by performing neutron powder diffraction studies on increasing temperature. Given the uncertainty over the solid solubility limit of Cs^+ in CuI (and its variation with temperature) and the difficulties in preparing homogeneously doped samples of sufficient size for neutron diffraction experiments ($\sim$few cm^3) the experiments were performed on a sample doped with 10% Cs^+. The excess Cs^+ forms the compound Cu_2CsI_3.[65]

Neutron powder diffraction studies of the $Cu_{1-x}Cs_xI$ sample were performed on the Polaris diffractometer at the ISIS spallation neutron source,[66] using a cylindrical sample of 6.0 mm diameter and 40 mm height, encapsulated under vacuum in a silica ampoule, and within a vanadium resistive heating furnace at temperatures up to $T=753(2)$ K. Data were collected using the time-of-flight method and the ZnS scintillator detector banks covering the scattering angles $83°\leqslant\pm 2\theta\leqslant 97°$. In addition, a two terminal measurement of the ionic conductivity was performed using a pellet of 5.0 mm diameter and 5.2 mm length held between two spring loaded platinum disks inside a boron nitride cell and inserted into the hot zone of a horizontal tube furnace. A Solartron S1260 Frequency Response Analyzer determined the conventional Z-Z' Bode plots over the frequency range from 10^{-1} to 10^7 Hz.

Two heating runs were carried out on the diffractometer. In the first, the inital mixture of CuI and CsI reacted at T

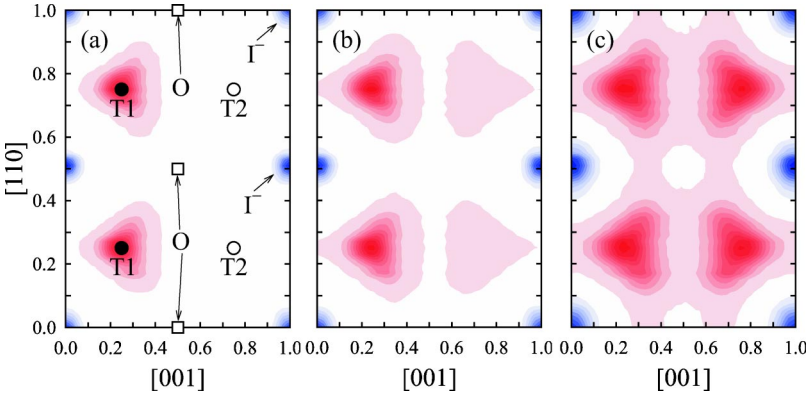

FIG. 8. (Color online) The simulated density of I^- and Cu^+ within the $(1\bar{1}0)$ plane of CuI at temperatures of (a) 600, (b) 660, and (c) 670 K. The I^- density is centered at 000 and $\frac{1}{2}\frac{1}{2}0$, etc. All other contours correspond to Ag^+ density. The densities are calculated within a slice of thickness 0.1 perpendicular to the plane. The locations of the octahedral (O) and tetrahedral ($T1$ and $T2$) sites are illustrated in plot (a).

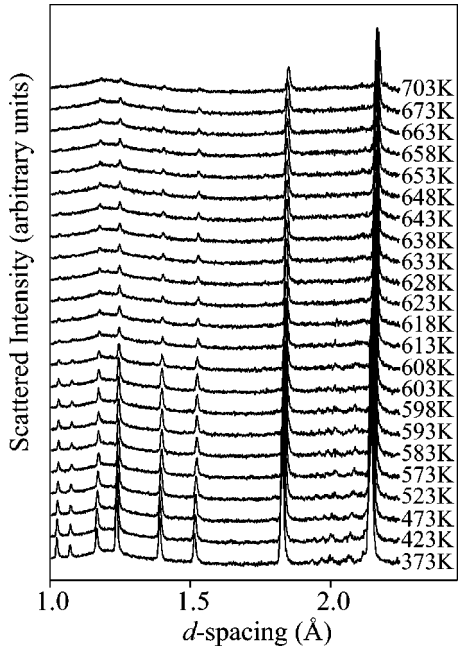

FIG. 9. The evolution of a portion of the powder neutron diffraction pattern collected on second heating of the $Cu_{1-x}Cs_xI$ sample.

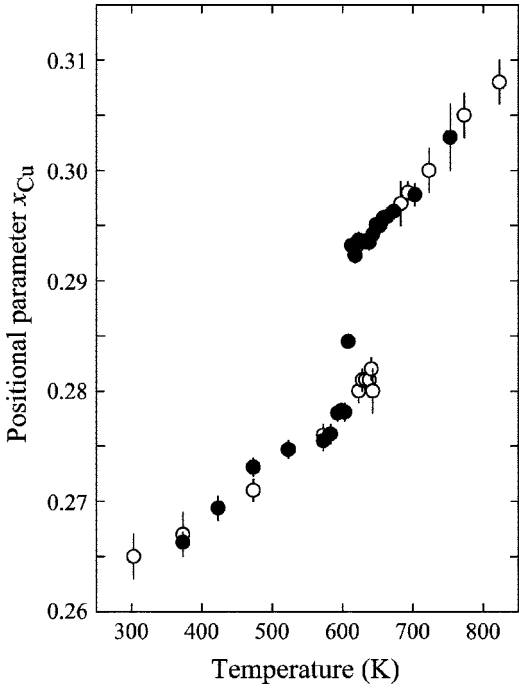

FIG. 10. The temperature dependence of the x parameter for Cu^+ ions in the tetrahedral sites in $Cu_{1-x}Cs_xI$ (filled circles) compared with pure CuI (Ref. 51) (open circles). In the γ-phase, Cu^+ are placed in 16*e* (*x*,*x*,*x*) positions, and in α-CuI, Cu^+ are in 32*f* (*x*,*x*,*x*) positions, both with $x \geqslant 0.25$ (in space groups $F\bar{4}3m$ and $Fm\bar{3}m$, respectively).

$\simeq$600 K to form $Cu_{1-x}Cs_xI$ and a residual amount of Cu_2CsI_3. On cooling and subsequent heating, the proportion of Cu_2CsI_3 remained constant. Both heating runs showed no reflections characteristic of the hexagonal β phase, thus confirming that this intermediate phase is not present in the $Cu_{1-x}Cs_xI$ sample (see Fig. 9). At $T=613(2)$ K there was a clear reduction in the intensities of the peaks of the $Cu_{1-x}Cs_xI$ phase, indicative of a direct (type-I) superionic transition between the γ and α phases. The data from the second heating run were refined using the Rietveld method and using the models described previously for CuI.[51] The results are summarized in Fig. 7 and 10.

The temperature variation of the volume per formula unit V/Z, as illustrated in Fig. 7(a), has an abrupt increase at the $\gamma \rightarrow \alpha$ transition at $T=608(3)$ K, and the values within both phases are, within error, the same as those for pure CuI. This indicates that the degree of the larger Cs^+ ion incorporated into the $Cu_{1-x}Cs_xI$ sample is very small, with $x<0.1\%$. The temperature variation of the ionic conductivity of $Cu_{1-x}Cs_xI$ is illustrated in Fig. 7(b). The general trend mirrors that observed in the MD simulations rather more closely than the behavior of pure CuI, with a gradual increase in σ within the γ phase leading to an abrupt rise at the transition to the α phase characterized by essentially constant σ. The increases in σ are clearly related to the small increases in Cu^+ occupation of the interstitial $T2$ site just below the $\gamma \rightarrow \alpha$ transition followed by complete disorder of Cu^+ ions over all $T1$ and $T2$ sites within the α phase [see Fig. 7(c)]. The anisotropic distribution of Cu^+ ions within the tetrahedral sites also closely follows the behavior of CuI (Ref. 51) (see Fig. 10 and Sec. IV for details). Hence, the structure of $Cu_{1-x}Cs_xI$ behaves in an analogous manner to that of CuI at high temperature, except that the hexagonal β phase has been suppressed and the $\gamma \rightarrow \alpha$ transition occurs at a slightly lower temperature.

IV. DISCUSSION

The suggestion that the $\gamma \rightarrow \alpha$ transition in CuI is a type-II superionic transition interrupted by the presence of the β phase[56,61] is not supported by either the MD simulation or experimental studies presented here. This clearly differs from the type-II behavior observed in the high pressure rocksalt structured phase AgI-III. The differences between the AgI-III and CuI cubic structures are a consequence of the unfavorable nature of the octahedral sites within CuI. In turn, this is a consequence of the greater degree of covalent bonding character within CuI (Ref. 67) and is demonstrated by the absence of a transition to the octahedrally coordinated rocksalt phase even at very high pressures.[68] Despite the implausibility, it is interesting to note that if the octahedral sites were available to the cations in CuI, then the superionic phases of both CuI and AgI-III would be very similar, with the disorder emerging from distinct ordered tetrahedrally and octahedrally coordinated structures, respectively.

The unavailability of the octahedral sites in CuI is not, in itself, sufficient to prevent the possibility of a type-II transition in γ-CuI. However, a small percentage of Cu^+ defects is sufficient to destabilize the fcc anion sublattice, either into the hcp β-phase (in the pure compound) or, if suitably constrained through doping or simulation, into an expanded fcc

structure, both via first-order phase transitions.

In order to understand this it is necessary to investigate the effect of a single Cu^+ moving from a $T1$ lattice site to a neighboring $T2$ interstitial site in γ-CuI. Since the concentration of defects is small, it is likely that this produces a local environment whereby the $T2$ interstitial Cu^+ has ~ 5 Cu^+ in neighboring $T1$ tetrahedra, all sharing edges with the, now filled, $T2$ tetrahedron. The separation between $T1$ and $T2$ sites is $a/2 \simeq 3.05$ Å whereas the observed separation between Cu^+ in α-CuI is just less than 2.7 Å.[50,63] This suggests that when neighboring tetrahedra are occupied in CuI, the Cu^+ ions are not at the centers of the tetrahedra, but rather that they are closer to each other. The average structure of γ-CuI at high temperature places Cu^+ in $16e$ (x,x,x) positions, with $x \simeq 0.28$ and in α-CuI, Cu^+ are in $32f$ (x,x,x) positions, with $x \simeq 0.3$, in space groups $F\bar{4}3m$ and $Fm\bar{3}m$, respectively[51] (see Fig. 10). These positions show that the anisotropic atomic displacements of Cu^+ cause them to move in $\langle 111 \rangle$ directions away from the neighboring I^- and towards the centers of the I^- tetrahedral faces. In order to satisfy the observed shortened nearest-neighbor Cu-Cu distance, the majority of nearest-neighbor Cu^+ must move in opposite directions, i.e., if a Cu^+ in $(\frac{1}{4},\frac{1}{4},\frac{1}{4})$ moves in $\langle 111 \rangle$ to (0.3,0.3,0.3) then a Cu^+ in $(\frac{3}{4},\frac{1}{4},\frac{1}{4})$ moves in $\langle \bar{1}11 \rangle$ to (0.7,0.2,0.2). This can become a collective motion within this local region and has the effect of destabilizing a layer of I^- ions as the defect concentration increases, thus inducing a structural phase transition. In contrast, the α phase is stable because the structure is completely disordered and less dense. Hence each Cu^+ ion has only three nearest neighbors on average and this, combined with the increased cell volume, does not produce a large enough distortion of the I^- sublattice to induce a phase transition.

The collective nature of Cu^+ motion within the γ phase has been observed in earlier MD studies, also noting that the mechanism is likely to be correlated to I^- motion.[54] It was argued that this induces a percolation transition between phases with low (i.e., the γ phase) and high (i.e., the α phase) diffusion when the number of correlated regions of diffusing Cu^+ ions is sufficient for them to interact. Since the percolation threshold for an fcc lattice is 0.12, then the maximum number of Cu^+ interstitials in the γ phase will be of this order. This picture is superficially consistent with the MD and diffraction results for $Cu_{1-x}Cs_xI$ reported here, although the γ-α transition is first order rather than the postulated second-order transition.[54] Also such a percolation transition cannot explain the fcc to hcp transition observed in pure CuI. Rather, it is the interaction of the Cu^+ interstitials with the I^- lattice that drives this phase transition.

In general therefore, superionic materials whose ''normal'' state has the zinc blende structure will tend to favor a type-I phase transition. This is because a small number of mobile tetrahedral defects will destabilise the immobile lattice to produce a structure based on a hcp lattice. This is true for CuCl, CuBr, and CuI and for related doped materials. Ag_2HgI_4 is a good example of this. Although there is a superionic transition between the cation ordered fcc β phase and cation disordered fcc α phase at $T = 326$ K, the disorder is only within the $T1$ sites and the $T2$ sites remain largely unoccupied.[69] The conductivity is fairly high ($\sigma \sim 10^{-4}\ \Omega^{-1}\,\mathrm{cm}^{-1}$)[70] because the $T1$ sites are only 75% filled. A further, more recent, study has shown that the true superionic ϵ phase ($\sigma \sim 10^{-1}\ \Omega^{-1}\,\mathrm{cm}^{-1}$), which has the α-AgI bcc structure, occurs at still higher temperatures via the hexagonal structured δ phase.[71]

The type-II superionic transition within AgI-III shows many similarities with the behavior of β-PbF_2,[4,6–10] especially the temperature dependence of many of the thermodynamic variables (V/Z, C_p and the defect concentration). Interestingly, high pressure has the opposite effect on PbF_2, since it favors a change to type-I superionic behavior because the more densely packed cotunnite structured α phase exhibits only minimal F^- Frenkel disorder on heating.[49] Clearly both AgI-III and β-PbF_2 sustain a type-II transition because their immobile sublattices are able to accommodate a large number of mobile defects. In AgI-III there are two additional tetrahedral interstices per Ag^+ and in β-PbF_2 there is considerable space (i.e., the octahedral voids) within the Pb^{2+} sublattice for the F^- defects.

V. CONCLUSIONS

This paper shows how the close combination of powder diffraction and MD simulation can be used to characterize superionic phase transitions effectively. This has been particularly effective because the measurements and the simulations were carried out at many temperatures across the phase transitions. Two transitions have been investigated in detail. The MD simulations of CuI, when constrained to remain cubic at all temperatures, clearly show a first-order transition between the ordered γ phase and superionic α phase, despite a small amount of Cu^+ disorder in γ-CuI just below the superionic transition. This has been supported by neutron diffraction data from CuI lightly doped with Cs^+ which has been shown to suppress the appearance of the hexagonal structured β phase. Hence it is argued that CuI does not have a ''hidden'' type-II transition. Instead, the phase transition is type I in character and it is proposed that this is a consequence of the destabilizing effect of a small percentage of tetrahedral Cu^+ defects on the I^- sublattice.

In contrast, high-pressure x-ray diffraction and MD simulations show that the high-pressure rocksalt structured AgI-III phase has a type-II superionic transition with very similar characteristics to those observed in β-PbF_2. Both AgI-III and β-PbF_2 are able to accommodate large number of mobile defects without distorting their immobile sublattices. The likelihood of a type-I or type-II transition to the superionic state is therefore critically dependent on the effect of the mobile defects on the immobile sublattice.

ACKNOWLEDGMENTS

The work presented in this paper forms part of a wider project investigating the structural properties of superionic conductors funded by the Engineering and Physical Sciences

Research Council (Grant No. GR/M38711). We are grateful to M. Mezuoar for assistance with the x-ray diffraction experiments performed at the ESRF. M.W. and D.A.K. thank the Royal Society and EPSRC, respectively, for financial support, and P.B. thanks the Swedish Research Council for financial support.

[1] S. Chandra, *Superionic Solids: Principles and Applications* (North Holland, Amsterdam, 1981).
[2] J.B. Boyce and B.A. Huberman, Phys. Rep. **51**, 189 (1979).
[3] M.T. Hutchings, K. Clausen, M.H. Dickens, W. Hayes, J.K. Kjems, P.G. Schnabel, and C. Smith, J. Phys. C **17**, 3903 (1984).
[4] J.P. Goff, W. Hayes, S. Hull, and M.T. Hutchings, J. Phys.: Condens. Matter **3**, 3677 (1991).
[5] M.J. Castiglione and P.A. Madden, J. Phys.: Condens. Matter **13**, 9963 (2001).
[6] A.B. Walker, M. Dixon, and M.J. Gillan, J. Phys. C **15**, 4061 (1982).
[7] R.B. Roberts and G.K. White, J. Phys. C **19**, 7167 (1986).
[8] T.S. Aurora, D.O. Pederson, and S.M. Day, Phys. Rev. B **41**, 9647 (1990).
[9] W. Schröter and J. Nölting, J. Phys. Colloid Chem. **41**, 6 (1980).
[10] N.H. Andersen, K. Clausen, and J.K. Kjems, Solid State Ionics **9-10**, 543 (1983).
[11] M.H. Dickens, W. Hayes, M.T. Hutchings, and C. Smith, J. Phys. C **15**, 4043 (1982).
[12] G. Burley, J. Chem. Phys. **38**, 2807 (1963).
[13] V.M. Nield and W. Hayes, Defect Diffus. Forum **125-126**, 37 (1995).
[14] P. Vashishta and A. Rahman, Phys. Rev. Lett. **40**, 1337 (1978).
[15] A.F. Wright and B.E.F. Fender, J. Phys. C **10**, 2261 (1977).
[16] V.M. Nield, D.A. Keen, W. Hayes, and R.L. McGreevy, Solid State Ionics **66**, 247 (1993).
[17] C. Tubandt and E. Lorenz, Z. Phys. Chem. (Leipzig) **87**, 513 (1914).
[18] V.M. Nield and D.A. Keen, *Diffuse Neutron Scattering from Crystalline Materials* (Oxford University Press, Oxford, 2001).
[19] V.M. Nield, R.L. McGreevy, D.A. Keen, and W. Hayes, Physica B **202**, 159 (1994).
[20] S. Hull, D.A. Keen, J. Phys.: Condens. Matter **8**, 6191 (1996).
[21] S. Hull, D.A. Keen, W. Hayes, and N.J.G. Gardner, J. Phys.: Condens. Matter **10**, 10 941 (1998).
[22] W. Bührer and W. Hälg, Electrochim. Acta **22**, 701 (1977).
[23] D.A. Keen, J. Phys.: Condens. Matter **14**, R819 (2002).
[24] N. Hainovsky and J. Maier, Phys. Rev. B **51**, 15 789 (1995).
[25] F. Zimmer, P. Ballone, J. Maier, and M. Parrinello, J. Chem. Phys. **112**, 6416 (2000).
[26] T. Ishii and O. Kamishima, J. Phys. Soc. Jpn. **70**, 158 (2001).
[27] V.M. Nield, D.A. Keen, W. Hayes, and R.L. McGreevy, J. Phys.: Condens. Matter **4**, 6703 (1992).
[28] W. Andreoni and M.P. Tosi, Solid State Ionics **11**, 49 (1983).
[29] O. Ohtaka, H. Takebe, A. Yoshiasa, H. Fukui, and Y. Katayama, Solid State Commun. **123**, 213 (2002).
[30] D.A. Keen and S. Hull, J. Phys.: Condens. Matter **5**, 23 (1993).
[31] B.-E. Mellander, Phys. Rev. B **26**, 5886 (1982).
[32] J.L. Tallon, Phys. Rev. Lett. **57**, 2427 (1986).
[33] J.L. Tallon, Phys. Rev. B **38**, 9069 (1988).
[34] C.A. Rains, J.R. Ray, and P. Vashishta, Phys. Rev. B **44**, 9228 (1991).
[35] D.A. Keen, S. Hull, W. Hayes, and N.J.G. Gardner, Phys. Rev. Lett. **77**, 4914 (1996).
[36] M. Mezouar, P. Faure, W. Crichton, N. Rambert, B. Sitaud, S. Bauchau, and G. Blattmann, Rev. Sci. Instrum. **73**, 3570 (2002).
[37] J.M. Besson, R.J. Nelmes, G. Hamel, J.S. Loveday, G. Weill, and S. Hull, Physica B **180&181**, 907 (1992).
[38] Y. Le Godec, D. Martinez-Garcia, M. Mezouar, G. Syfosse, J.P. Itie, and J.M. Besson, High Press. Res. **17**, 35 (2000).
[39] A.P. Hammersley, S.O. Svensson, M. Hanfland, A.N. Fitch, and D. Haüsermann, High Press. Res. **14**, 235 (1996)
[40] B.E. Warren, *X-ray Diffraction* (Addison-Wesley, Reading, MA, 1969).
[41] R.L. McGreevy, J. Phys.: Condens. Matter **13**, R877 (2001).
[42] M. Parrinello, A. Rahman, and P. Vashishta, Phys. Rev. Lett. **50**, 1073 (1983).
[43] P.A. Madden, K.F. O'Sullivan, and G. Chiarotti, Phys. Rev. B **45**, 10 206 (1992).
[44] C. Seok and D.W. Oxtoby, Phys. Rev. B **56**, 11 485 (1997).
[45] C. Seok and D.W. Oxtoby, Phys. Rev. B **58**, 5146 (1998).
[46] K. O'Sullivan, G. Chiarotti, and P.A. Madden, Phys. Rev. B **43**, 13 536 (1991).
[47] G.E. Murch, Solid State Ionics **7**, 177 (1982).
[48] K. Ihata and H. Okazaki, J. Phys.: Condens. Matter **9**, 1477 (1997).
[49] M.J. Castiglione, M. Wilson, P.A. Madden, and C.P. Grey, J. Phys.: Condens. Matter **13**, 51 (2001).
[50] A. Chahid and R.L. McGreevy, J. Phys.: Condens. Matter **10**, 2597 (1998).
[51] D.A. Keen and S. Hull, J. Phys.: Condens. Matter **7**, 5793 (1995).
[52] D.A. Keen and S. Hull, J. Phys.: Condens. Matter **6**, 1637 (1994).
[53] J.X.M. Zheng-Johansson, I. Ebbsjö, and R.L. McGreevy, Solid State Ionics **82**, 115 (1995).
[54] J.X.M. Zheng-Johansson and R.L. McGreevy, Solid State Ionics **83**, 35 (1996).
[55] R.L. McGreevy and J.X.M. Zheng-Johansson, Solid State Ionics **95**, 215 (1997).
[56] S. Miyake, S. Hoshino, and T. Takenaka, J. Phys. Soc. Jpn. **7**, 19 (1952).
[57] J.B. Wagner and C.J. Wagner, J. Chem. Phys. **26**, 1597 (1957).
[58] J.B. Boyce and B.A. Huberman, Solid State Commun. **21**, 31 (1977).
[59] G. Burns, F.H. Dacol, and M.W. Shafer, Solid State Commun. **24**, 753 (1977).
[60] A. Rahman and P. Vashishta, in *The Physics of Superionic Conductors and Electrode Materials*, edited by J. W. Perram, Vol. 92 of *NATO Advanced Studies Institute Series B: Physics* (Plenum Press, 1980), p. 93.
[61] M.B. Salamon in *Physics of Superionic Conductors*, edited by M.B. Salamon, Vol. 15 of *Topics in Current Physics* (Springer Verlag, Berlin, 1979), p. 175.
[62] J. Trullàs, A. Giró, R. Fonatanet, and M. Silbert, Phys. Rev. B **50**, 16 279 (1994).

[63] A. Trapananti, A. Di Cicco, and M. Minicucci, Phys. Rev. B **66**, 014202 (2002).
[64] T. Matsui and J.B. Wagner, J. Electrochem. Soc. **124**, 300 (1977).
[65] N. Jouini, L. Guen, and M. Tournoux, Rev. Chim. Mineral. **17**, 486 (1980).
[66] S. Hull, R.I. Smith, W.I.F. David, A.C. Hannon, J. Mayers, and R. Cywinski, Physica B **180&181**, 1000 (1992).
[67] J.C. Phillips, Rev. Mod. Phys. **42**, 317 (1970).
[68] M. Hofmann, S. Hull, and D.A. Keen, Phys. Rev. B **51**, 12 022 (1995).
[69] S. Hull and D.A. Keen, J. Phys.: Condens. Matter **12**, 3751 (2000).
[70] S. Hull, D.A. Keen, and P. Berastegui, J. Phys.: Condens. Matter **14**, 13 579 (2002).
[71] S. Hull and D.A. Keen, J. Phys.: Condens. Matter **13**, 5597 (2001).